

1 **Title:** Ectopical expression of bacterial collagen-like protein
2 supports its role as adhesin in host-parasite coevolution

3

4 **Authors**

5 Benjamin Huessy^{1,2}, Dirk Bumann² & Dieter Ebert¹

6

7 ¹ University of Basel, Department of Environmental Sciences, Zoology, Vesalgasse 1, 4051 Basel,
8 Switzerland

9 ² University of Basel, Biozentrum, Spitalstrasse 41, 4056 Basel, Switzerland

10

11 Corresponding authors:

- 12 • Benjamin Huessy (benjamin.huessy@gmail.com)
13 • Dieter Ebert (dieter.ebert@unibas.ch)

14

15 orCID:

16 Benjamin Huessy 0000-0002-3193-4231

17 Dirk Bumann 0000-0003-3636-4239

18 Dieter Ebert 0000-0003-2653-3772

19

20

21 Running Title: *Pasteuria* collagen-like protein is an adhesin to its host

22

23 Key words: *Daphnia magna*, *Pasteuria ramosa*, collagen-like proteins, host-parasite interactions, fusion
24 protein, *Bacillus thuringiensis*

25

26

27

28 **Abstract**

29 For a profound understanding of the mechanisms of antagonistic coevolution, it is necessary to identify
30 the coevolving genes. The spore-forming bacterium *Pasteuria ramosa* and its host, the microcrustacean
31 *Daphnia*, are a well-characterized paradigm for co-evolution, but the underlying genes remain largely
32 unknown. A genome-wide association study identified a polymorphic carboxy-terminal globular domain
33 of *Pasteuria* collagen-like protein 7 (Pcl7) as a candidate mediating parasite attachment and driving its
34 coevolution with the host. Since *P. ramosa* cannot currently be genetically manipulated, we used *Bacillus*
35 *thuringiensis* as a surrogate parasite to express a fusion protein of a Pcl7 carboxy-terminus from *P.*
36 *ramosa* and the amino-terminal domain of a *B. thuringiensis* collagen-like protein. Mutant *B.*
37 *thuringiensis* (Pcl7-*Bt*) spores but not wild-type *B. thuringiensis* (WT-*Bt*) spores, attached to the same site
38 of susceptible hosts as *P. ramosa*. Furthermore, Pcl7-*Bt* spores attached readily to host genotypes that
39 were susceptible to the *P. ramosa* clone that was the origin of the Pcl7 C-terminus, but only slightly to
40 resistant host genotypes. These findings indicated that the fusion protein was properly expressed and
41 folded and demonstrated that indeed the C-terminus of Pcl7 mediates attachment in a host genotype-
42 specific manner. These results provide strong evidence for the involvement of a CLP in the coevolution of
43 *Daphnia* and *P. ramosa* and opens new avenues for genetic epidemiological studies of host-parasite
44 interactions.

45 **150-word "Importance" paragraph**

46 During host-parasite coevolution, hosts evolve to evade the damaging effect of the parasite, while
47 parasites evolve to maximize their benefits by exploiting the host. The genes underlying this coevolution
48 remain largely unknown. For the prime model-system for coevolutionary research, the crustacean
49 *Daphnia* and the parasite *Pasteuria ramosa*, collagen-like proteins (CLPs) in *Pasteuria* were suggested to
50 play a crucial role for host-parasite interactions. Here we report that transferring part of a CLP coding
51 gene from the unculturable *P. ramosa* to *Bacillus thuringiensis* (*Bt*), confirmed the function of this protein
52 as a genotype-specific adhesin to the host's cuticle. Our finding highlights the importance of a CLP in
53 host-parasite interactions and will enable us to explore the population genetic dynamics of coevolution in
54 this system.

55

56

57 Introduction

58 Antagonistic coevolution between hosts and parasites has been suggested to be a major driver in
59 evolution, presumably underlying diverse biological phenomena, such as the extraordinary genetic
60 variation at the major histocompatibility complex (MHC) of jawed vertebrates and R-genes in plants, the
61 parasite hypothesis about the evolution of sexual selection, the evolution of genetic recombination and the
62 evolution of immune systems (1–3). While great progress has been made in our understanding of
63 coevolution and its consequences at the phenotypic level, much less is known about the underlying
64 genetics (4–6). However, current theories about the mechanism of coevolution are genetic models, such
65 as the selective sweep model, where new beneficial mutations sweep to fixation in both antagonists, and
66 balancing selection models, where alleles at specific loci interact in a manner that generates negative
67 frequency dependent selection (7, 8). Therefore, to test these models and understand the evolutionary
68 dynamics during coevolution, we need to identify the genes involved in host-parasite interactions. This is
69 particularly challenging in non-model systems, where genetic tools are largely lacking.

70 A prime model system for coevolution research is the water flea *Daphnia* and the bacterial parasite
71 *Pasteuria ramosa*. *P. ramosa* is a highly virulent obligate parasite of its planktonic crustacean host. It
72 cannot be cultured outside its host. For the *Pasteuria*–*Daphnia* system, coevolutionary dynamics have
73 been demonstrated in natural and experimental settings, with negative frequency dependent selection
74 being the main explanation for the observed dynamics (9–11). The system is renowned for its strong
75 genotypic infection specificity (12–14), but the genes responsible for this specificity have not been
76 identified, even so candidates have been suggested for both host and parasite (15–17). During infection,
77 dormant *P. ramosa* endospores are taken up by the filter-feeding *Daphnia* and shed their exosporium,
78 revealing numerous peripheral fibres (13). These activated spores attach to the cuticles of susceptible
79 *Daphnia*, most commonly to the oesophagus or the hindgut wall (15, 18, 19). The current understanding
80 is that the peripheral fibres of the activated spores may be collagen-like proteins (CLPs) that act as
81 adhesins on surface components on the *Daphnia* epithelium.

82 Collagen-like proteins (CLPs), proteins with high similarity to eukaryotic collagens, have been identified
83 in a range of prokaryotes (20–22) including human-pathogenic species such as *Bacillus anthracis* (23),
84 *Legionella pneumophila* (24) and several *Streptococcus* species (25). CLPs typically attach to cell walls
85 (26, 27) and contain a rod-shaped collagenous domain near the cell surface (28–30). Research on bacterial
86 CLPs indicates that they play a pivotal role in host–pathogen interactions during the initial stages of
87 infection for attachment to host cells and surfaces (31–36). While most bacteria contain only a few genes
88 that encode for CLPs (21), the endospore-forming bacteria of the Gram-positive *Pasteuria* genus carries

89 up to 50 CLP-encoding genes (20, 37), one of them, Pcl7 of *P. ramosa*, was suggested to be responsible
90 for the highly specific interaction with the host and may play an important role in their coevolution (19).
91 Conducting a genome-wide-association study Andras et al. (19) discovered multiple phenotype-associated
92 sequence polymorphisms in the *P. ramosa pcl7* gene encoding for a *Pasteuria* collagen-like protein,. In
93 its C-terminal domain (CTD), *pcl7* contains seven single-nucleotide sequence polymorphisms that
94 correlate perfectly with infection phenotype and that encompass considerable changes in the size,
95 hydrophobicity, and charge of the respective amino acids. These findings suggest that Pcl7 may be crucial
96 for spore–host attachment and, furthermore, that sequence variation in Pcl7 may be important for
97 determining the high specificity of the bacterial spore’s adhesion to the host epithelium in the oesophagus.
98 The aim of this study was to test the hypothesis that *pcl7* is responsible for attachment to the host's
99 oesophagus through experimental manipulation of Pcl7.

100 Genetic engineering on *P. ramosa* has not yet been successful because its rigid exosporium resists lysis
101 and degradation (38), preventing us from generating *pcl7* mutants. However, CLPs can be engineered in
102 the *Bacillus cereus* group (39–43), providing a heterologous system for studying *pcl7* and other *Pasteuria*
103 factors (44). BclA, a structural homolog of Pcl7 (19) is part of the exosporium in the entire *B. cereus*
104 group including *B. thuringiensis*, a species with well-developed techniques for laboratory experiments.
105 Members of the *B. cereus* group develop spores encapsulated by an exosporium composed of two defined
106 layers (29): a primary basal layer and an outermost hair-like structure (45, 46). BclA makes up the
107 majority of this hair-like structure (23). It is expressed at the spore surface late during sporulation and
108 requires the specific amino acid sequence motif “LVGPTLPPIPP” for incorporation into the exosporium
109 (47).

110 Here, we used the collagen-part of BclA as a display platform for the CTD of Pcl7 in *B. thuringiensis* to
111 obtain a surrogate parasite that displays the key part of Pcl7 on its surface. Analogous display systems
112 have already been used to express functional fusion proteins (48–50). We showed that the Pcl7 CTD
113 mediated attachment of the surrogate parasite spores to the oesophagus wall of *D. magna* and that this
114 single protein part was sufficient to recapitulate host genotype specificity of the donor *P. ramosa* clone.
115 These data demonstrate the key role of Pcl7 CTD in this paradigmatic host-pathogen system.

116

117 Material and Methods

118 Table 1. Material used in the study

119 A. *Daphnia magna* genotypes (=clones) used in the study

Clone	Country of Origin (collection site)	C1 Resistotype
HU-HO-2	Hungary	Susceptible
NO-AA-1	Norway	Susceptible
RU-AST1-1	Russia	Susceptible
CH-H-2016-h-34	Switzerland	Susceptible
FI-Xinb3	Finland	Resistant
DE-G1-106	Germany	Resistant

120 Table 1A: Six *D. magna* clones with different resistance phenotypes to the C1 *P. ramosa* clone were maintained in
 121 artificial culture medium (ADaM) under standard laboratory conditions (20 °C, 16:8 day:night cycle, *Tetrademus*
 122 *obliquus* as food) as previously described in (51).

123

124 B. Bacterial strains and plasmids used in this study

Strain or plasmid	Characteristics	Reference
Bacterial strain		
<i>B. thuringiensis</i> 407 Cry	AcrySTALLiferous <i>B. thuringiensis</i> strain	(52)
<i>E. coli</i> DC10B	<i>mcrA</i> Δ (<i>mrr-hsdRMS-mcrBC</i>) ϕ 80 <i>lacZ</i> Δ M15 Δ <i>lacX74</i> <i>recA1</i> <i>araD139</i> Δ (<i>ara-leu</i>)7697 <i>galU</i> <i>galK</i> <i>rpsL</i> <i>endA1</i> <i>nupG</i> Δ <i>dcm</i>	(53)
<i>P. ramosa</i> C1 and C19	cloned lines of <i>P. ramosa</i> , isolated from natural populations	(13)
Plasmid		
pBKJ223	Plasmid encoded homing restriction enzyme I-SceI, promoting the second (54) homologous recombination event in procedure for making markerless deletion mutant, Tet ^r	
pMAD-I-SceI	Plasmid used for making deletion mutants, containing I-SceI restriction site that can be cleaved by the homing endonuclease I-SceI, Apr, Eryr	(55)

125

126 **Media**

127 *E. coli* DC10B was cultured in lysogenic broth (LB) (10 g/L bacto tryptone, 5 g/L yeast extract, 10 g/L
128 NaCl) medium. *B. thuringiensis* was cultured in tryptic soy broth (TSB) (30 g/L bacto tryptic soy broth)
129 medium. LB-lowsalt (LB-ls) (10 g/L bacto tryptone, 5 g/L yeast extract, 5 g/L NaCl) was used to prepare
130 electrocompetent cells. For electroporation, Super-Optimal broth with Catabolite Repression (SOC) (20
131 g/L tryptone, 5 g/L yeast extract, 0.5 g/L NaCl, 4.8 g/L MgSO₄, 0.186 g/L KCl, and 3.6 g/L glucose) was
132 used. For selection, we used LB agar plates (10 g/L bacto tryptone, 5 g/L yeast extract, 10 g/L NaCl, 15
133 g/L agar) and TSB agar plates (30 g/L bacto tryptic soy broth, 15 g/L agar) with erythromycin at a final
134 concentration of 5 µg/mL, ampicillin at a final concentration of 100 µg/mL, and anhydrous tetracycline at
135 a final concentration of 8 µg/mL.

136 **Preparation of electrocompetent cells and electroporation**

137 To prepare electrocompetent cells, 100 mL of fresh LB-ls was inoculated at OD_{600nm} 0.01 from an
138 overnight culture and grown to OD_{600nm} 0.08 at 37 °C, 180 rpm. The culture was distributed to two 50-mL
139 falcon tubes and put on ice for 20 min. The tubes were spun down at 4 °C, 8000 rpm for 8 min, and the
140 supernatant was removed. The pellets were then washed with 30 mL cold sterile water containing 15 %
141 glycerol (AppliChem, A1123,1000), and the tubes were spun down at 4 °C, 8000 rpm for 8 min. This
142 washing step was repeated twice. The supernatant was discarded, and the pellet was suspended in 1 mL
143 cold sterile water containing 15 % glycerol. Finally, 100 µL aliquots were stored at -80 °C or used
144 directly for electroporation.

145 For electroporation of plasmid DNA, DNA (100 ng) was added to thawed, electrocompetent cells (100
146 µL) in a 1-mm electroporation cuvette on ice. For *E. coli* DC10B, a single pulse at 1.8 V (Gene Pulser
147 Xcell Electroporation Systems, Bio-Rad Laboratories) was applied. For *B. thuringiensis*, a single pulse at
148 2.5 V was applied. Immediately after the pulse, 900 µL of pre-warmed SOC media was added, and the
149 entire volume was transferred to a fresh 1.5-mL Eppendorf tube. The tube was incubated and shaken at 37
150 °C, 180 rpm for 1 h. Samples were spun down for 4 min at 11000 rpm. We removed 900 µL of
151 supernatant and plated the remaining volume (100 µL) on LB agar containing the respective antibiotics.
152 Plates were incubated overnight at 37 °C.

153

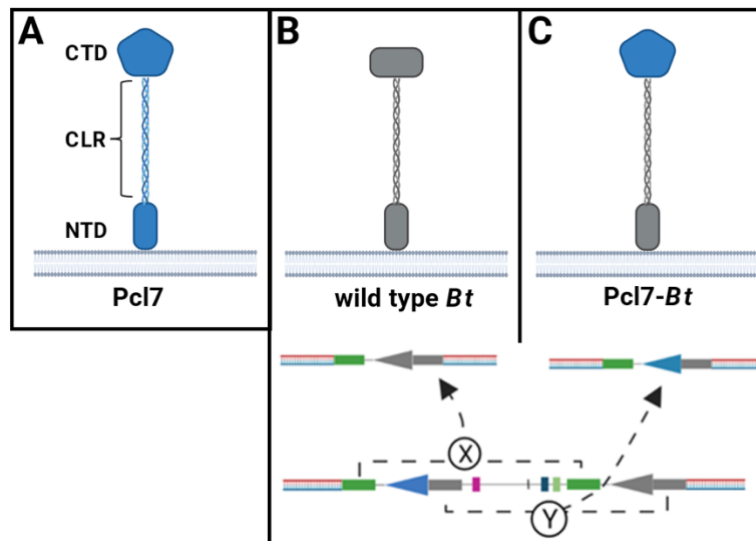
154

155 Isolation of genomic DNA

156 Genomic DNA was isolated using a DNeasy Blood & Tissue Kit (Qiagen GmbH, Hilden, Germany). A 2-
157 mL overnight culture of *B. thuringiensis* in TSB media was spun down at 8.000 rpm for 4 min. The
158 supernatant was discarded, and the pellet was resuspended in 200 μ L AL Buffer and 20 μ L of proteinase
159 K. The sample was incubated at 56 $^{\circ}$ C, 500 rpm for 10 min, and 200 μ L >99 % ethanol was added to it. It
160 was then mixed thoroughly, transferred to a DNeasy Mini spin column, and spun down at 10000 rpm for
161 1 min; the flow through was discarded. 500 μ L of Buffer AW1 was then added and spun down at 10000
162 rpm for 1 min, and the flow through was discarded. Finally, 500 μ L of Buffer AW2 was added and spun
163 down at 13200 rpm for 1 min. The column was transferred to a fresh 1.5-mL Eppendorf tube, and the
164 DNA was eluted with 50 μ L sterile water, incubated at room temperature for 1 min and centrifuged at
165 10000 rpm for 30 sec. The concentration of DNA was measured using a Colibri Microvolume
166 Spectrometer (Berthold Technologies, Bad Wildbad, Germany).

167

168 Figure 1. Graphic overview of the construction of the Pcl7-Bt fusion



169 (A) Pcl7 consists of three domains: an amino-terminal (NTD), a central collagen-like region (CLR) and a carboxy-
170 terminal globular domain (CTD). (B) Homologous recombination can occur either through homologous regions
171 “X”, resulting in the regeneration of the wild type gene and protein, (C) or through “Y”, resulting in the generation
172 of the Pcl7-Bt fusion. Figure created with Biorender.com.

173

174

175 **Molecular Biology**

176 Plasmids were constructed by Gibson Assembly (56). Flanking regions (~750 bp) of the target locus were
177 PCR-amplified from genomic DNA (with primers 1 & 2 as well as 5 & 6, Table 2) using Phanta Max
178 Super-Fidelity DNA Polymerase (Vazyme Biotech, Nanjing, China), and primers were designed with
179 SnapGene (v. 5.2, Gibson assembly tool). The 501 bp C-terminal *pcl7* sequence was synthesized
180 (LubioScience GmbH, Zurich, Switzerland), and PCR-amplified using primers 3 & 4. The pMAD-I-SceI
181 vector was amplified with primers 7 & 8 in a long-range PCR. The resulting three fragments and the
182 vector were fused using the Hifi DNA Assembly Master Mix (New England Biolabs, Ipswich, USA) at
183 50 °C for 1 h. The reaction mix contained approximately 40 ng of each fragment and 150 ng of vector for
184 a total volume of 20 µL. *E. coli* DC10B was transformed with the resulting product. Plasmid DNA was
185 purified from an overnight culture using a plasmid miniprep kit (ZymoPURE, ZymoResearch). Sequence-
186 verified plasmids were electroporated into *B. thuringiensis*. Cells were incubated at 28 °C for 1 h and
187 plated on TSB agar containing 5 µg/mL erythromycin.

188 The allelic-exchange procedure was done as described (54) with some modifications. *B. thuringiensis*
189 integrants were isolated by shifting transformants obtained by electroporation from 28 °C to 37 °C in the
190 presence of 5 µg/mL erythromycin. pMAD-I-SceI cannot replicate in *B. thuringiensis* at 37 °C, so only
191 cells which integrated the plasmid into the chromosome could propagate. Colonies were screened for the
192 orientation of their insert using PCR (with primers 9 & 10, Table 2). Colonies that harboured the right-
193 hand insert were pooled and inoculated in 4 mL fresh TSB medium containing 5 µg/mL erythromycin at
194 37 °C, 180 rpm overnight. The overnight culture was diluted 1:100 in 50 mL fresh TSB medium
195 containing 5 µg/mL erythromycin and incubated at 37 °C, 180 rpm to an OD_{600nm} of 0.8 to prepare
196 electrocompetent cells. The cells were transformed with pBKJ223 and plated on TSB agar containing 8
197 µg/mL tetracycline. Colonies were pooled and inoculated in 4 mL fresh TSB medium containing 8 µg/mL
198 tetracycline at 37 °C, 180 rpm for 6 h. Serial dilutions (10⁻¹, 10⁻², 10⁻³, 10⁻⁴) were prepared and 100 µL of
199 each dilution was plated on TSB agar plates containing 8 µg/mL tetracycline. Single colonies were
200 patched on TSB agar with 8 µg/mL tetracycline as well as TSB agar with 5 µg/mL erythromycin to screen
201 for loss of erythromycin-resistance. Erythromycin-sensitive clones were picked and stored in 50 µL LB-
202 Glycerol (15 %) at -20 °C. The clones were screened for the desired insert (Fig 1C; recombination
203 through homologous regions “Y”) using primers 9 & 10. Clones with confirmed allelic exchange were
204 inoculated into 4 mL fresh TSB media and incubated at 37 °C, 180 rpm overnight. Genomic DNA was
205 prepared and Sanger-sequenced (Microsynth AG, Balgach, Switzerland). Correct clones were inoculated
206 in 4 mL fresh TSB and incubated at 37 °C, 180 rpm overnight. The next day freezer stocks were
207 generated and stored at -80 °C for later use.

208 **Table 2. Primers used in this study**

	Primer name	Sequence 5' → 3'
1	pBH01_F1.FOR	AATTCAGCACTTGCTCCTGCTGGAAG
2	pBH01_F1.REV	TAGACAGATCTATCGATGCATGCCATGGTATCAACATAATCACCCCTCTTCCAAATCAATC A
3	pBH01_F2.FOR	TTCTACTGCTAAGTAAAAAATTATTTTATTTTCTAATAGTAATATAACTATCAATAGGAC TATATGG
4	pBH01_F2.REV	GGACTTCCAGCAGGAGCAAGTGCTGAA
5	pBH01_F3.FOR	ATATCGGATCCATATGACGTCGACGCGTCTTTTACTTGATCATTTAGTAAATCATATTTTT TAAAATTCTCTTGTACTTG
6	pBH01_F3.REV	CTATTAGAAAAATAAAAATAATTTTTACTTAGCAGTAGAACTGTTATCAGTTTTACT
7	pBH01_Vector.FOR	AGATGACGACCATCAGGGACAG
8	pBH01_Vector.REV	AGTGTAAGAGAGTTGATAAATGATTATATTGGGAC
9	pBH04_Gen.rev	CAATATAAAGGTTTCCCGTTAGAATCCATCGCAAGAT
10	pBH04_Gen.fwd	CACCTACATATTGGACGAGTTCAGGAGG

209

210 **Sporulation and purification of spores**

211 Spores were purified as described by (57) with some modifications. An overnight culture of *B.*
212 *thuringiensis* in 4 mL of TSB was grown at 37 °C, 180 rpm. The overnight culture was diluted 1:100 in
213 50 mL fresh TSB media containing 0.1 mmol MnSO₄ (PanReac, AppliChem) and grown at 37 °C, 180
214 rpm for 10 days. Cultures were transferred to a 50-ml falcon tube and stored on ice for 20 min. The tubes
215 were spun down at 4 °C, 10000 rpm for 10 min. The pellet was suspended in 20 mL of 50 mM Tris-HCL
216 (ph 7.2; PanReac, AppliChem) with an addition of 50 µg/mL lysozyme (from hen egg whites, Fluka).
217 Samples were incubated at 37 °C, 180 rpm for 1 h. The sample was spun down at 4 °C, 10000 rpm for 10
218 min, and the pellet was suspended in cold sterile water. This washing step was repeated twice. The pellet
219 was then suspended in 5 mL 0.05 % SDS solution (Sigma, D6750-10G) by vortexing and incubated for 5
220 min at room temperature. The sample was then spun down at 4 °C, 10000 rpm for 10 min, and the pellet
221 was suspended in cold sterile water. This washing step was repeated five times. After the final washing
222 step, the pellet was suspended in 5 mL of cold, sterile water and stored at 4 °C for later use. Spores were
223 counted using a Neubauer improved chamber (Paul Marienfeld GmbH, Lauda-Konigshofen, Germany)
224 with a chamber depth of 0.1 mm.

225 **Fluorescent labelling of spores**

226 *Pasteuria ramosa* spores were isolated by homogenizing infected *Daphnia* in ADaM followed by
227 centrifugation at room temperature, 8000 rpm for 5 min. *Bacillus thuringiensis* spores were thawed and
228 centrifuged at room temperature, 8000 rpm for 5 min. *P. ramosa* or *B. thuringiensis* pellets were
229 suspended in 0.8 mL of 0.1 M sodium bicarbonate (pH 9.1; Sigma, S5761-500G) with 2 mg/mL of
230 fluorescein-5(6)-isothiocyanate (Sigma-Aldrich, Miss, USA). The samples were then incubated in the
231 dark at room temperature, 1600 rpm shaking for 2 h, followed by centrifugation at room temperature,
232 8000 rpm for 4 min. The pellet was suspended in 0.8 mL sterile water and centrifuged at room
233 temperature, 8000 rpm for 4 min; the supernatant was then removed. This washing step was repeated
234 three times. Spore suspensions were stored in sterile water at 4 °C in the dark for further use.

235 **Attachment assay**

236 *Daphnia* were individually placed into a 96 well plates containing 150 µL of ADaM per well. 10 µL of
237 spore solution containing ~ 500 fluorescently labelled *P. ramosa* spores were added to each well and
238 incubated in the dark for 5 min. For *B. thuringiensis*, 10 µL of spore solution containing ~ 50'000 labelled
239 *B. thuringiensis* spores were added to each well and incubated in the dark for 5 min. The entire liquid
240 volume in each well was removed and replaced with 150 µL fresh ADaM. This washing step was
241 repeated twice, after which the entire liquid volume in each well was removed. The *Daphnia* were placed
242 individually on a microscopy slide using a toothpick. A glass cover slide was applied to the *Daphnia*
243 gently to avoid crushing it. Extended focus images were taken using Leica Application Suite (v. 4.12,
244 using package “montage”) with a Leica DM6 B (Leica Microsystems, Wetzlar, Germany) microscope
245 fitted with a Leica DFC 7000T camera and a GFP Filter cube (Excitation Filter BP 470/40).

246 **Competitive attachment assay**

247 *Daphnia* were individually placed into a 96-well plate containing 150 µL of ADaM per well. We then
248 added 10 µL of spore solution to each well according to each treatment—for C1/C19: 50 labelled *P.*
249 *ramosa* spores; for WT-*Bt* + C1/C19: ~ 20'000 labelled *B. thuringiensis* spores followed by 50 labelled *P.*
250 *ramosa* spores; and for Pcl7-*Bt* + C1/C19: ~ 20'000 labelled Pcl7-*Bt* spores followed by 50 labelled *P.*
251 *ramosa* spores—and incubated them in the dark for 5 min. The entire liquid volume in each well was
252 removed and replaced with 150 µL fresh ADaM. This washing step was repeated twice to remove excess
253 spores. The *Daphnia* were then placed individually on a microscopy slide and a glass cover slide was

254 gently applied to the *Daphnia* to avoid crushing them. The number of *P. ramosa* spores attached to the *D.*
255 *magna* oesophagus were then counted by manually scanning the z-stacks.

256 Selection of candidate collagen-like proteins

257 The N-terminal domain and collagen-like region of three out of eight *bclA* homologs in *B. thuringiensis*
258 (Table 3) were selected based on their similar length and sequence as *pcl7* to construct fusions with the
259 *pcl7* CTD.

260

261 Table 3. Candidate collagen-like proteins in *B. thuringiensis*

262 Locus tag	262 Product	262 Reasoning	262 Motif
BTB_c12600	Collagen-like exosporium surface protein	Short and highly similar NTD to <i>pcl7</i>	LVGPTLPPIPP
BTB_c35490	Collagen triple helix repeat protein	Similar NTD to <i>pcl7</i>	LIGPTLPSIPP
BTB_c38740	Triple helix repeat-containing collagen	Similar NTD to <i>pcl7</i>	IIGPTLPPVPP

262

263 Table 3: Three candidate *B. thuringiensis* genes with similar N-terminal domains and amino acid sequences as *pcl7*.
264 Deviations from the specific sequence motif, likely required for incorporation into the exosporium, are marked in
265 bold. Sequences were obtained from GenBank (58)(accession no. CP003889).

266

267 Results

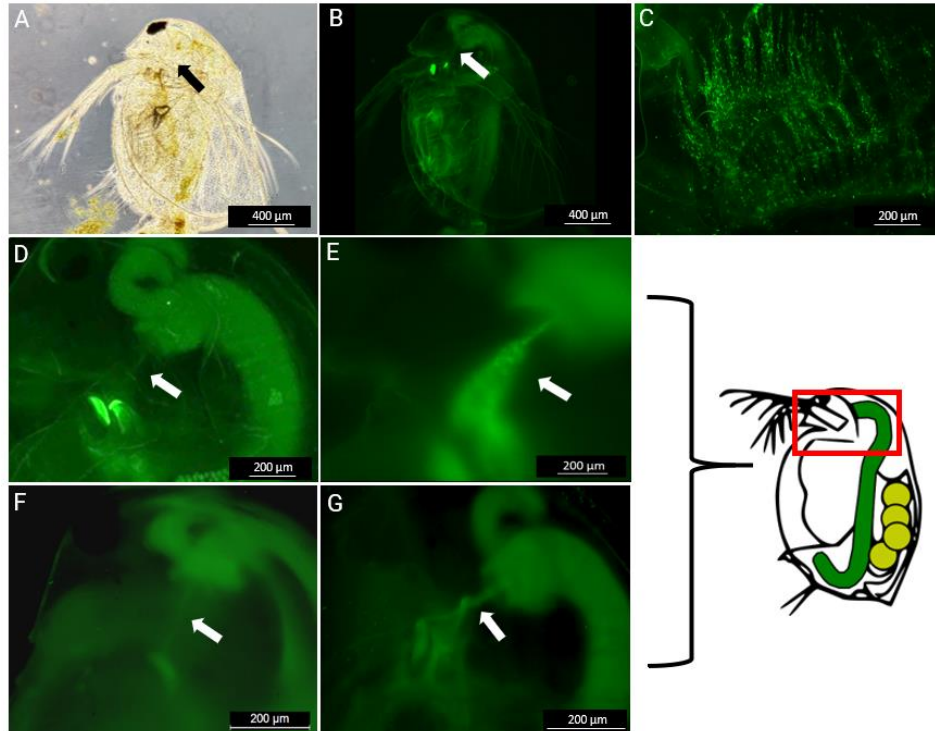
268 To validate the role of the C-terminal domain (CTD) of the collagen-like protein Pcl7 of *Pasteuria*
269 *ramosa* as an adhesin that recognizes the host *Daphnia magna* in a genotype-specific manner, we
270 employed surface presentation on *Bacillus thuringiensis* spores. Specifically, we fused the Pcl7-CTD to
271 the N-terminal domain of the main collagen-like exosporium surface protein of *B. thuringiensis*
272 (BTB_c12600, Table 3). Compared to other potential fusion partners with collagen-like domain
273 (BTB_c35490, BTB_c38740, Table 3) BTB_c12600 is more similar in its N-terminal collagen-like
274 domain to Pcl7 and contains a peptide that matches perfectly to the consensus motif for incorporation in
275 the surface exosporium. We identified the CTD of BTB_c12600 in *Bt* 407 as the N-terminal 166 amino
276 acids after the last collagen-like repeat unit (Table 4). We replaced this CTD in the chromosome of *Bt* 407
277 with the 167 amino acid-long CTD of Pcl7 using two consecutive single cross-overs. The construct was

278 verified by sequencing. The resulting recombinant Pcl7-*Bt* strain showed normal growth and sporulation.
 279 We induced spore formation and purified spores using standard procedures.
 280

281 **Table 4. Amino acid sequences used for the Pcl7-*Bt* fusion**

Protein	Amino acid sequence	Length
<i>Bt</i> 407 BTB_c12600	MSNNNYSNGLNPDESLSASAFDNLVGP TLPPIPPFTLPTGPTGPTGPTGPTGPTVP TGPTGPTGPTGPTGPTGPTGPTGPTGPTGDTGTTGPTGPTGDTGATGPTGPTGDT GATGPTGPTGDTGATGPTGPTGDTGATGPTGPTGDTGATGPTGPTGATGPTGPT GPSGLGLPAGLYAFNSAGISLDLGLNAPVPFNTVGSQFGTAISQLDADTFVIAETG FYKITVIVYTA AISVLGGLTIQVNGVSVPGTGATLISVGAPIVVQAITQITTTPSLVE VIVTGLGLSLALGTNASIIIKVA*	305 AA
Pcl7	MMSILVGP TGPTGPTGDTGVPGGAIGITGPTGQSMTGIMGNQGSPGIQGPTGITGI TGPTGITGITGISITGPTGTTGFTGITGPTGVTGPTGETGPVIFISGITGPTGPTGP TGVNITGSTGITGSQGITGNTGLQGPQGPQISPGPSGIQGNQGP IGT ASAEIASFRR FTLANVTTFTTPVNFNSQFNLS SSSISLLSNNTDISIQPGTYIFNFGGLLYSAGGGGA GANESAVYLSLVSGSLNTYGTNIKQPYGFAS TLTRQNTSASAYGYGGMLYQVAE YMIQV TAAAVIRMLLFNASSYTMTPAQLMLPYSPIDSYITIRKIK*	331 AA
Pcl7- <i>Bt</i> fusion	MSNNNYSNGLNPDESLSASAFDNLVGP TLPPIPPFTLPTGPTGPTGPTGPTGPTVP TGPTGPTGPTGPTGPTGPTGPTGPTGPTGDTGTTGPTGPTGDTGATGPTGPTGDT GATGPTGPTGDTGATGPTGPTGDTGATGPTGPTGDTGATGPTGPTGATGPTGPT ASAEIASFRRFTLANVTTFTTPVNFNSQFNLS SSSISLLSNNTDISIQPGTYIFNFGGLL YSAGGGGAGANESAVYLSLVSGSLNTYGTNIKQPYGFAS TLTRQNTSASAYGYG GMLYQVAEYMIQV TAAAVIRMLLFNASSYTMTPAQLMLPYSPIDSYITIRKIK*	333 AA

282 Table 4: Amino acid sequences of the native *Bt* collagen-like exosporium surface protein BTB_c12600, the Pcl7
 283 protein and the resulting Pcl7-*Bt* fusion protein. The *Bt* NTD used in the fusion protein is highlighted in grey, the
 284 Pcl7 CTD in light blue. The * represents the stop codon.



285

286 **Figure 2. Attachment phenotypes using labelled spores**

287 Microscopy images of the various attachment phenotypes using labelled spores. The red box in the schematic to the
288 right indicates the approximate area (head region) of images D-G. (A) Bright field image of a *D. magna* (genotype
289 (=clone) HU-HO-2) showing the entire animal with an arrow indicating the site of the oesophagus. (B) Overview of
290 a *D. magna* (genotype HU-HO-2) using a GFP Filter cube showing the entire animal with an arrow indicating the
291 location of the oesophagus. Note the weak autofluorescence of the *D. magna* tissue. (C) Labeled *B. thuringiensis*
292 vegetative cells accumulated in the filter setae of a *D. magna* (genotype HU-HO-2). (D) Closeup of the *D. magna*
293 foregut with arrow indicating the position of the oesophagus, situated perpendicular to the arrow. The two bright
294 objects left of the arrow are the autofluorescent mandibles. (E) Upper body of a susceptible *D. magna* (genotype
295 HU-HO-2) with labelled C1 *P. ramosa* spores attached to the oesophagus (arrow). (F) Upper body of a resistant *D.*
296 *magna* (genotype FI-Xinb3) where labelled Pcl7-Bt spores do not aggregate in the oesophagus (arrow). The faint
297 visible light fluorescent band is attributed to autofluorescence. The beginning of the mid gut, visible in the upper
298 right corner, shows fluorescence because labelled spores have been ingested by the *Daphnia*. (G) Upper body of a
299 susceptible *D. magna* (genotype HU-HO-2) with labelled Pcl7-Bt spores attached to the oesophagus (arrow). The
300 midgut with its appendix (=caecum) is visible on the right.

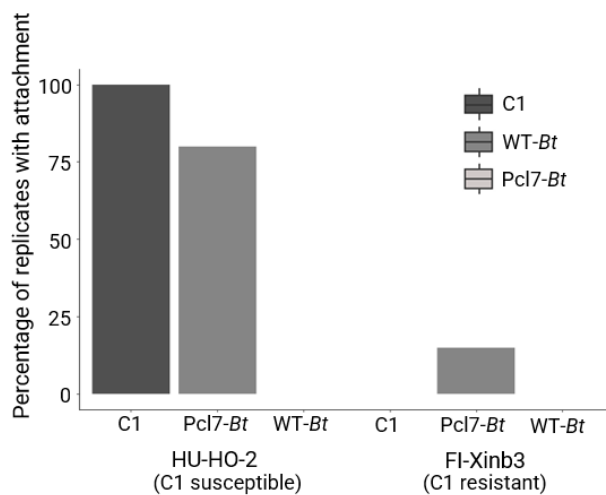
301

302 To determine adherence of *P. ramosa* and wild type (WT-Bt) or *pcl7*-expressing (Pcl7-Bt) *B.*
303 *thuringiensis* spores to *D. magna*, we covalently labelled the bacteria with fluorescein and tracked them in

304 infection assays with different *D. magna* genotypes using fluorescence microscopy (13). C1 *P. ramosa*
305 spores attached to the oesophagus of susceptible *D. magna* (Fig. 2E; 100 % attachment, Fig. 3) but not to
306 resistant hosts (Fig. 3) as previously observed. Vegetative WT-*Bt* and Pcl7-*Bt* cells showed no attachment
307 to the *D. magna* oesophagus but can be observed in the filter setae of both susceptible and resistant
308 *Daphnia* (Fig. 2C), possibly being trapped in the mucus that lines the filter feeding apparatus. WT-*Bt*
309 spores showed attachment neither to the susceptible nor resistant host (0% attachment, Fig. 3), while
310 Pcl7-*Bt* spores attached to the oesophagus of susceptible *D. magna* (Fig 2G). Pcl7-*Bt* attached at low
311 frequency and density to resistant *D. magna* (Fig. 2F; 15 % attachment, Fig. 3), possibly suggesting
312 incorrect glycosylation of Pcl7 (19) in the heterologous *B. thuringiensis* system. Attachment of Pcl7-*Bt*
313 spores to other tissues or known sites of *P. ramosa* attachment such as the hindgut or the external post-
314 abdomen (59) was not observed. Thus, a single domain of collagen-like protein from *P. ramosa* was
315 sufficient to mediate *Pasteuria*-like adhesion properties for recombinant *B. thuringiensis* spores.

316

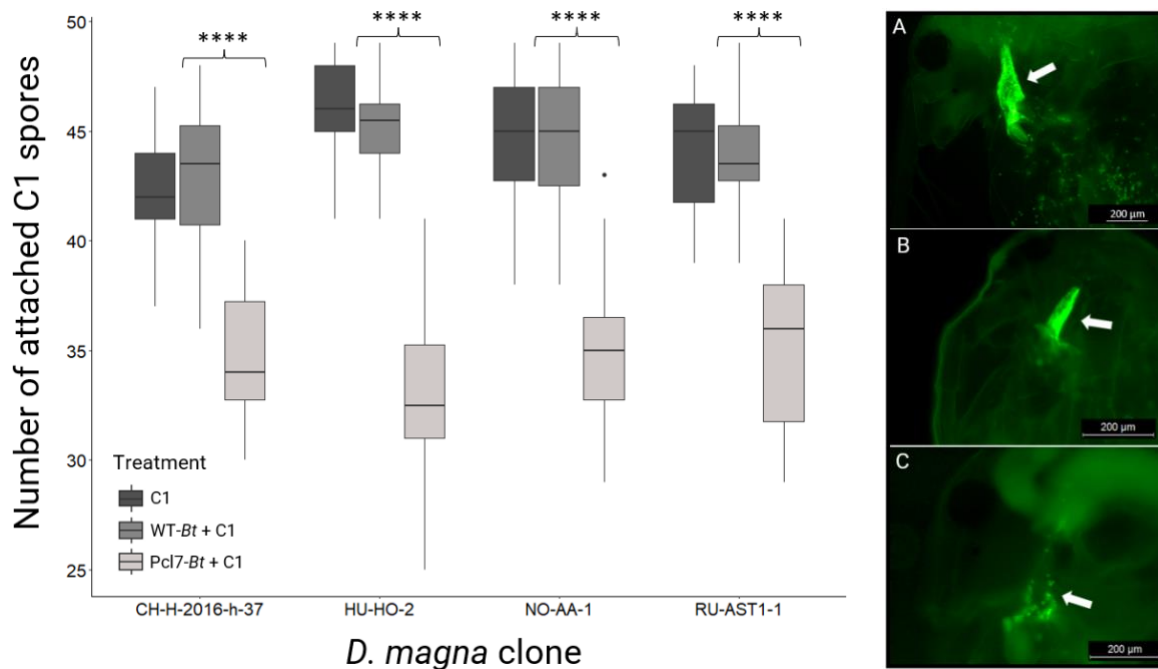
317 **Figure 3. Attachment assay**



318 *D. magna* that are both susceptible (genotype HU-HO-2) and resistant (genotype FI-Xinb3) to C1 *P. ramosa* were
319 exposed to different bacteria: around 5000 labelled C1 *P. ramosa* spores (“C1”), ~50’000 labelled *B. thuringiensis*
320 WT-*Bt* spores (“WT-*Bt*”), or ~50’000 labelled Pcl7-*Bt* spores (“Pcl7-*Bt*”). Each isolate was tested on 20 host
321 individuals for each resistotype (N=20, 120 individuals in total).

322

323 **Figure 4. Competitive attachment assay for C1 *P. ramosa***



324 “C1”– Individuals were exposed to 50 labelled C1 *P. ramosa* spores (picture **A**); “WT-Bt + C1” –Individuals were
325 exposed to ~20’000 *B. thuringiensis* WT-Bt spores prior to the addition of 50 C1 *P. ramosa* spores (**B**); “Pcl7-Bt +
326 C1” – Individuals were exposed to ~20’000 Pcl7-Bt spores prior to the addition of 50 C1 *P. ramosa* spores (**C**).
327 Each treatment was performed using 20 individual *D. magna*, and the assay was repeated for four different host
328 genotypes (N = 20, 60 individuals per genotype (=clone), 240 individuals in total). A t-test was performed to
329 compare the WT-Bt + C1 against Pcl7-Bt + C1 means. **** means the t-test is significant with a p-value < 10⁻⁸. The
330 boxplots display the 25th percentile, median and 75th percentile, while the whiskers display the minimum (Q1-
331 1.5*IQR) and maximum (Q3+1.5*IQR). Outliers are shown as dots. Statistical analysis was done using R (V. 4.1.0,
332 with the R-base package and R packages “ggubr” and “ggplot2”).

333

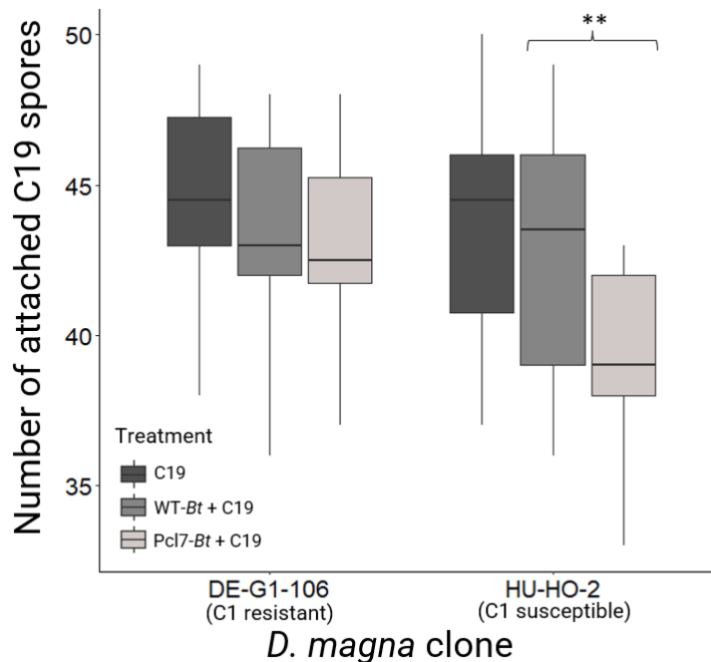
334 To determine if Pcl7 presented on *B. thuringiensis* spores can block *P. ramosa* adhesion to *D. magna*, we
335 infected various *D. magna* genotypes with 50 spores of two different *P. ramosa* clones after incubation
336 with a 400-fold excess of the much smaller WT-Bt or Pcl7-Bt spores. After 5 min exposure, we counted
337 the number of *P. ramosa* spores attaching to the *D. magna* oesophagus. WT-Bt had no impact on
338 subsequent *P. ramosa* adhesion for all tested *D. magna* and *P. ramosa* genotypes (Fig. 4). However, Pcl7-
339 Bt diminished adhesion of C1 *P. ramosa* spores in four different susceptible *D. magna* genotypes,
340 indicating that Pcl7 was sufficient to block adhesion sites in the host for *P. ramosa*.

341 We also tested Pcl7-Bt against C19 *P. ramosa* that show a different host genotype dependence than C1 *P.*
342 *ramosa* (the source of Pcl7 in Pcl7-Bt). Pcl7-Bt had no impact on C19 adhesion to *D. magna* DE-G1-106

343 (susceptible to *P. ramosa* C19; resistant to C1), but diminished C19 adhesion to *D. magna* HU-HO-2
344 (susceptible to *P. ramosa* C19 and susceptible to C1) (Fig. 5). Thus, Pcl7-Bt could prevent *P. ramosa*
345 adhesion specifically in *D. magna* resistotypes with a Pcl7-receptor (enabling infection by C1), but not in
346 *D. magna* resistotypes without such a receptor. As C19 uses a different receptor than C1, the blocking in
347 HU-HO-2 was probably mediated by steric hindrance between adhering Pcl7-Bt and *P. ramosa*.

348

349 **Figure 5. Competitive attachment assay for C19 *P. ramosa***



350 “C19” – Individuals were exposed to 50 labelled C19 *P. ramosa* spores; “WT-Bt + C19” – Individuals were exposed
351 to ~20’000 WT-Bt spores prior to the addition of 50 C19 *P. ramosa* spores; “Pcl7-Bt + C19” – Individuals were
352 exposed to ~20’000 Pcl7-Bt spores prior to the addition of 50 C19 *P. ramosa* spores. Each treatment was performed
353 using 20 individual *D. magna*, and the assay was repeated for two different genotypes (N = 20, 60 individuals per
354 genotype, 120 individuals in total). ** *t*-test, $p < 0.01$.

355

356

357 Discussion

358 The mechanism underlying specific coevolution by negative frequency-dependent selection is believed to
359 be driven by the interaction between host and parasite genes. Identifying these genes marks a major step

360 towards understanding this mechanism. In the *Daphnia* - *Pasteuria* system coevolution is well
361 characterized on a phenotypic level, but the underlying genes are still largely unknown. Here we tested
362 and confirmed the hypothesis that a collagen-like protein (CLP) is crucial for the attachment of the
363 *Pasteuria* parasite to the cuticle of its *Daphnia* host. Polymorphism in the attachment phenotype had
364 previously been shown to be the most important step in the coevolution of the two antagonists (13, 18),
365 and a specific CLP (Pcl7) of *P. ramosa* was linked to the attachment polymorphism (19). Here we used *B.*
366 *thuringiensis* as a surrogate to express a functional fusion protein harbouring the globular domain of Pcl7.
367 By replacing a single C-terminal sequence in *B. thuringiensis* with the one from *Pasteuria* Pcl7, we were
368 able to create *B. thuringiensis* spores capable of attaching *in vivo* to the host's oesophagus wall. This
369 result is in line with previous studies that have sought to understand CLP function in bacterial infections
370 using deletion mutants for CLPs (60) or purifying recombinant CLPs (35). Our Pcl7-*Bt* spores not only
371 attached well to four susceptible host genotypes (Figs. 3, 4), but they also attached only sparsely to two
372 resistant host genotypes (Figs. 3, 5), revealing a very similar specificity to that of *P. ramosa* (Fig. 6).

373 Proteins associated with the spore coat in *B. thuringiensis*, including the BclA homologs that were altered
374 in this study, are predominantly synthesized during sporulation (43). We anticipated that the Pcl7 fusion
375 protein would be present upon completed spore formation. Consistent with this, only spores but not
376 vegetative Pcl7-*Bt* cells adhered to the host's oesophagus. The specificity of the *B. thuringiensis* spores to
377 a single host tissue thus indicates the functional ectopical expression of the Pcl7 fusion protein, generating
378 the same attachment phenotype as C1 *P. ramosa* spores. This attachment specificity was only seen in
379 hosts susceptible to C1 *P. ramosa*, while in two resistant host genotypes, attachment was either weak or
380 entirely absent. Thus, by replacing part of a single protein, we were able to transform *B. thuringiensis*
381 from non-attaching to attaching, recreating the first step of the infection process. To test if Pcl7-*Bt* spores
382 adhere to the same molecular structure in the oesophagus wall as C1 *P. ramosa* spores we conducted
383 competitive attachment assays. We found that the moieties or potential receptors on the *D. magna*
384 oesophagus cuticle surface are blocked by the Pcl7-*Bt* spores, supporting our hypothesis that the Pcl7-*Bt*
385 interferes with the attachment sites of C1 *P. ramosa*.

386 The specificity of the Pcl7-*Bt*'s attachment was less pronounced than that of the original *P. ramosa*
387 pathogen, with the difference in attachment between a resistant and a susceptible host genotype being 0 %
388 and 100 % for C1 *P. ramosa*, while it was 15 % and 80 % for the Pcl7-*Bt* spores (Fig. 3). Furthermore,
389 the competitive attachment assays showed that C1 spores were not totally blocked from attachment. Some
390 *Pasteuria* spores were still able to attach after the host had been treated with the Pcl7-*Bt* spores. Finally,
391 to see a visible picture of attachment, we needed much higher spore concentrations of the Pcl7-*Bts* than
392 the bigger *P. ramosa* pathogen. However, the weak signals observed are certainly caused in part by the

393 rapid germination of *B. thuringiensis* spores once exposed to the *Daphnia*, as germinating spores do not
394 express BclA (43). Furthermore, because *P. ramosa* spores are large (about 5.5 µm diameter) and thus
395 much more visible compared to the *B. thuringiensis* spores (about 1.6 x 0.8 µm) (61), more spores are
396 required to see attachment with the fluorescent microscope.

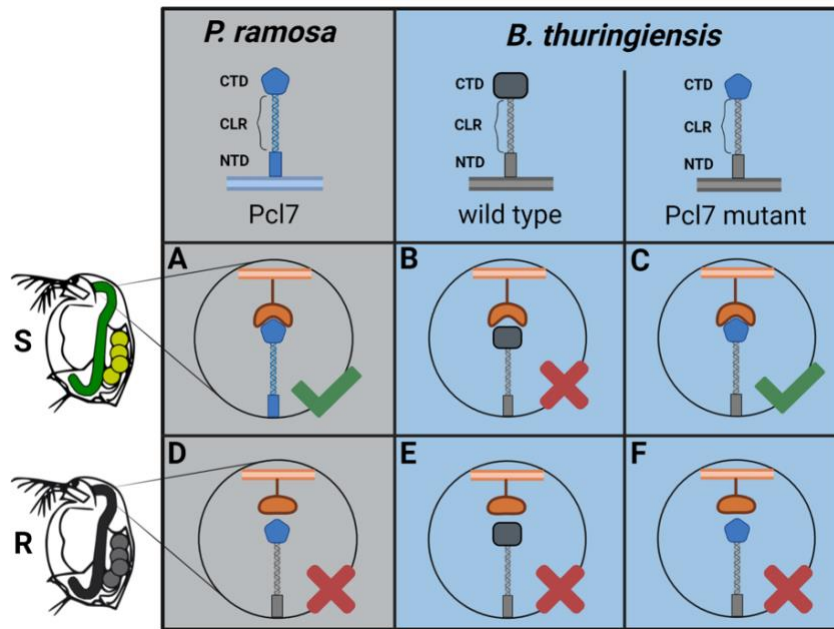
397 Other factors, not considered here, may contribute to spore attachment. One such factor may be
398 glycosylation. BclA, and CLPs in general, are known to be highly glycosylated (62, 63). The sequence
399 polymorphism of Pcl7 results in two predicted N-linked glycosylation sites, one of which correlates with
400 the infection phenotype of *Pasteuria* (19) and thus may partly explain the attachment polymorphism. The
401 Pcl7 fusion protein expressed in *B. thuringiensis* may contain different glycans than Pcl7 expressed in *P.*
402 *ramosa* or might not be glycosylated at all. This might result in altered adhesion properties. Other fusion
403 proteins containing other sequence polymorphisms or glycosylation sites might be used in the future to
404 work out the details of these differences. An analysis of the specific carbohydrate moieties of the Pcl7
405 glycoprotein could also be done to support this hypothesis (64). However, our data show that such a
406 potential mis-glycosylation had an only a minor impact on adhesion and competition.

407 Our study verified that the globular part of the Pcl7 protein contributes decisively to the parasite's ability
408 to attach to the host cuticle, although the molecular mechanisms for the attachment polymorphism are still
409 unclear, as is the composition of the host cuticle surface in the oesophagus. Previous research has shown
410 that CLPs can bind to a variety of molecules and cell surface components such as integrins (28),
411 glycoproteins (34), polysaccharides (65), lipoproteins (35) and mammalian collagen (66). Future studies
412 could focus on identifying the *D. magna* receptor for Pcl7.

413

414

415 **Figure 6. Proposed mechanism for Pcl7-mediated attachment**



416

417 (A) C1 *P. ramosa* ectopically expresses Pcl7 and attaches to the oesophagus of susceptible (S) *D. magna* by binding
 418 to host cell surface moieties. (B) WT-*Bt* spores do not attach to the oesophagus of susceptible *D. magna* due to the
 419 lack of a compatible moiety on the host cell surface. (C) Pcl7-*Bt* spores, harbouring the Pcl7 fusion protein attach to
 420 the oesophagus of susceptible *D. magna* by binding to the same cell surface moieties as the original Pcl7. (D) C1 *P.*
 421 *ramosa* does not attach to the oesophagus of resistant (R) *D. magna*. (E) WT-*Bt* spores and (F) Pcl7-*Bt* spores do
 422 not attach to the oesophagus of resistant *D. magna*. Figure created with Biorender.com

423

424

425

426

427 **Acknowledgements**

428 We thank J. Hottinger, U. Stiefel, M. Krebs, B. Claudi and members of the Bumann group for help in the laboratory.
 429 We thank members of the Ebert group for feedback on the study and the manuscript. We thank S. Zweizig for
 430 language editing. We thank Prof. Dr. Ole Andreas Økstad from the Department of Pharmacy of the University of
 431 Oslo, Norway for providing the strain and two plasmids used for markerless gene replacement in this study. This
 432 work was supported by the Swiss National Science Foundation (SNSF) (grant numbers 310030B_166677,
 433 310030_188887 to D.E.).

434

435 **Author contributions.**

436 All authors conceived the study. B.H. conducted the laboratory work and analyzed the results. All authors discussed
 437 the results. B.H. wrote the manuscript, which was read, edited and approved by all authors.

438

439 **Competing interests.**

440 All authors declare no competing interests.

441

442
443
444
445
446
447
448
449
450
451
452
453
454
455
456
457
458
459
460
461
462
463
464
465
466
467
468
469
470
471
472
473
474
475
476
477
478
479
480
481
482
483
484
485
486
487
488
489
490
491

References

1. Jack R, Du Pasquier L. 2019. *Evolutionary Concepts in Immunology*. Springer Nature Switzerland.
2. Poulin R. 2007. *Evolutionary ecology of parasites*. Princeton University Press, Princeton, USA.
3. Schmid-Hempel P. 2021. *Evolutionary Parasitology*, 2nd edition. Oxford University Press, Oxford, UK.
4. Ebert D, Fields PD. 2020. Host–parasite co-evolution and its genomic signature. *Nat Rev Genet* 21:754–768.
5. Vorburger C, Perlman SJ. 2018. The role of defensive symbionts in host–parasite coevolution. *Biol Rev* 93:1747–1764.
6. Thrall PH, Barrett LG, Dodds PN, Burdon JJ. 2016. Epidemiological and Evolutionary Outcomes in Gene-for-Gene and Matching Allele Models. *Front Plant Sci* 6.
7. Woolhouse MEJ, Webster JP, Domingo E, Charlesworth B, Levin BR. 2002. Biological and biomedical implications of the co-evolution of pathogens and their hosts. *Nat Genet* 32:569–577.
8. Ebert D. 2018. Open questions: what are the genes underlying antagonistic coevolution? *BMC Biol* 16:114.
9. Ameline C. 2020. Evolution and genetic architecture of resistance in a natural population of *Daphnia magna* undergoing strong epidemics of the bacteria *Pasteuria ramosa*. PhD thesis. University of Basel.
10. Auld SKJR, Tinkler SK, Tinsley MC. 2016. Sex as a strategy against rapidly evolving parasites. *Proc R Soc B-Biol Sci* 283.
11. Decaestecker E, Gaba S, Raeymaekers JAM, Stoks R, Van Kerckhoven L, Ebert D, De Meester L. 2007. Host–parasite ‘Red Queen’ dynamics archived in pond sediment. *Nature* 450:870–873.
12. Bento G, Routtu J, Fields PD, Bourgeois Y, Du Pasquier L, Ebert D. 2017. The genetic basis of resistance and matching-allele interactions of a host-parasite system: The *Daphnia magna*-*Pasteuria ramosa* model. *PLOS Genet* 13:e1006596.
13. Duneau D, Luijckx P, Ben-Ami F, Laforsch C, Ebert D. 2011. Resolving the infection process reveals striking differences in the contribution of environment, genetics and phylogeny to host-parasite interactions. *BMC Biol* 9:11.
14. Luijckx P, Fienberg H, Duneau D, Ebert D. 2013. A Matching-Allele Model Explains Host Resistance to Parasites. *Curr Biol* 23:1085–1088.
15. Bento G, Fields PD, Duneau D, Ebert D. 2020. An alternative route of bacterial infection associated with a novel resistance locus in the *Daphnia*–*Pasteuria* host–parasite system. *Heredity* 1–11.
16. Fredericksen M, Fields PD, Du Pasquier L, Ricci V, Ebert D. 2023. QTL study reveals candidate genes underlying host resistance in a Red Queen model system. *PLOS Genet* 19:e1010570.
17. McElroy K, Mouton L, Du Pasquier L, Qi W, Ebert D. 2011. Characterisation of a large family of polymorphic collagen-like proteins in the endospore-forming bacterium *Pasteuria ramosa*. *Res Microbiol* 162:701–714.
18. Ebert D, Duneau D, Hall MD, Luijckx P, Andras JP, Du Pasquier L, Ben-Ami F. 2016. A Population Biology Perspective on the Stepwise Infection Process of the Bacterial Pathogen *Pasteuria ramosa* in *Daphnia*, p. 265–310. *In Advances in Parasitology*. Elsevier.
19. Andras JP, Fields PD, Du Pasquier L, Fredericksen M, Ebert D. 2020. Genome-Wide Association Analysis Identifies a Genetic Basis of Infectivity in a Model Bacterial Pathogen. *Mol Biol Evol* 37:3439–3452.
20. Mouton L, Traunecker E, McElroy K, Pasquier LD, Ebert D. 2009. Identification of a polymorphic collagen-like protein in the crustacean bacteria *Pasteuria ramosa*. *Res Microbiol* 8.
21. Qiu Y, Zhai C, Chen L, Liu X, Yeo J. 2021. Current Insights on the Diverse Structures and Functions in Bacterial Collagen-like Proteins. *ACS Biomater Sci Eng* acsbiomaterials.1c00018.
22. Xu C, Yu Z, Inouye M, Brodsky B, Mirochnitchenko O. 2010. Expanding the Family of Collagen Proteins: Recombinant Bacterial Collagens of Varying Composition Form Triple-Helices of Similar Stability. *Biomacromolecules* 11:348–356.
23. Sylvestre P, Couture-Tosi E, Mock M. 2002. A collagen-like surface glycoprotein is a structural component of the *Bacillus anthracis* exosporium. *Mol Microbiol* 45:169–178.

- 492 24. Vandersmissen L, De Buck E, Saels V, Coil DA, Anné J. 2010. A *Legionella pneumophila* collagen-like protein
493 encoded by a gene with a variable number of tandem repeats is involved in the adherence and invasion of
494 host cells. *FEMS Microbiol Lett* 306:168–176.
- 495 25. Lukomski S, Bachert BA, Squeglia F, Berisio R. 2017. Collagen-like proteins of pathogenic streptococci:
496 Streptococcal collagen-like proteins. *Mol Microbiol* 103:919–930.
- 497 26. Rasmussen M, Jacobsson M, Björck L. 2003. Genome-based Identification and Analysis of Collagen-related
498 Structural Motifs in Bacterial and Viral Proteins. *J Biol Chem* 278:32313–32316.
- 499 27. Thompson BM, Stewart GC. 2008. Targeting of the BclA and BclB proteins to the *Bacillus anthracis* spore
500 surface. *Mol Microbiol* 70:421–434.
- 501 28. Humtsoe JO, Kim JK, Xu Y, Keene DR, Höök M, Lukomski S, Wary KK. 2005. A Streptococcal Collagen-like
502 Protein Interacts with the $\alpha 2\beta 1$ Integrin and Induces Intracellular Signaling. *J Biol Chem* 280:13848–13857.
- 503 29. Kailas L, Terry C, Abbott N, Taylor R, Mullin N, Tzokov SB, Todd SJ, Wallace BA, Hobbs JK, Moir A, Bullough
504 PA. 2011. Surface architecture of endospores of the *Bacillus cereus*/anthracis/thuringiensis family at the
505 subnanometer scale. *Proc Natl Acad Sci* 108:16014–16019.
- 506 30. Sylvestre P, Couture-Tosi E, Mock M. 2003. Polymorphism in the Collagen-Like Region of the *Bacillus*
507 anthracis BclA Protein Leads to Variation in Exosporium Filament Length. *J Bacteriol* 185:1555–1563.
- 508 31. Bozue J, Moody KL, Cote CK, Stiles BG, Friedlander AM, Welkos SL, Hale ML. 2007. *Bacillus anthracis* Spores
509 of the bclA Mutant Exhibit Increased Adherence to Epithelial Cells, Fibroblasts, and Endothelial Cells but Not
510 to Macrophages. *Infect Immun* 75:4498–4505.
- 511 32. Brahmhatt TN, Janes BK, Stibitz ES, Darnell SC, Sanz P, Rasmussen SB, O’Brien AD. 2007. *Bacillus anthracis*
512 Exosporium Protein BclA Affects Spore Germination, Interaction with Extracellular Matrix Proteins, and
513 Hydrophobicity. *Infect Immun* 75:5233–5239.
- 514 33. Wang Y, Jenkins SA, Gu C, Shree A, Martinez-Moczygemba M, Herold J, Botto M, Wetsel RA, Xu Y. 2016.
515 *Bacillus anthracis* Spore Surface Protein BclA Mediates Complement Factor H Binding to Spores and
516 Promotes Spore Persistence. *PLOS Pathog* 25.
- 517 34. Caswell CC, Han R, Hovis KM, Ciborowski P, Keene DR, Marconi RT, Lukomski S. 2008. The Scl1 protein of M6-
518 type group A *Streptococcus* binds the human complement regulatory protein, factor H, and inhibits the
519 alternative pathway of complement. *Mol Microbiol* 67:584–596.
- 520 35. Han R, Caswell CC, Lukomska E, Keene DR, Pawlowski M, Bujnicki JM, Kim JK, Lukomski S. 2006. Binding of
521 the low-density lipoprotein by streptococcal collagen-like protein Scl1 of *Streptococcus pyogenes*. *Mol*
522 *Microbiol* 61:351–367.
- 523 36. Karlstrom A, Jacobsson K, Flock M, Flock J, Guss B. 2004. Identification of a novel collagen-like protein, SclC,
524 in using signal sequence phage display. *Vet Microbiol* 104:179–188.
- 525 37. McElroy K, Mouton L, Du Pasquier L, Qi W, Ebert D. 2011. Characterisation of a large family of polymorphic
526 collagen-like proteins in the endospore-forming bacterium *Pasteuria ramosa*. *Res Microbiol* 162:701–714.
- 527 38. Stewart GC. 2015. The Exosporium Layer of Bacterial Spores: a Connection to the Environment and the
528 Infected Host. *Microbiol Mol Biol Rev* 79:21.
- 529 39. Sylvestre P, Couture-Tosi E, Mock M. 2002. A collagen-like surface glycoprotein is a structural component of
530 the *Bacillus anthracis* exosporium. *Mol Microbiol* 45:169–178.
- 531 40. Boydston JA, Chen P, Steichen CT, Turnbough CL. 2005. Orientation within the Exosporium and Structural
532 Stability of the Collagen-Like Glycoprotein BclA of *Bacillus anthracis*. *J Bacteriol* 187:5310–5317.
- 533 41. Gohar M, Gilois N, Graveline R, Garreau C, Sanchis V, Lereclus D. 2005. A comparative study of *Bacillus*
534 *cereus*, *Bacillus thuringiensis* and *Bacillus anthracis* extracellular proteomes. *PROTEOMICS* 5:3696–3711.
- 535 42. Waller LN, Stump MJ, Fox KF, Harley WM, Fox A, Stewart GC, Shahgholi M. 2005. Identification of a Second
536 Collagen-Like Glycoprotein Produced by *Bacillus anthracis* and Demonstration of Associated Spore-Specific
537 Sugars. *J Bacteriol* 187:4592–4597.
- 538 43. Peng Q, Kao G, Qu N, Zhang J, Li J, Song F. 2016. The Regulation of Exosporium-Related Genes in *Bacillus*
539 *thuringiensis*. *Sci Rep* 6:19005.
- 540 44. Srivastava A, Mohan S, Davies KG. 2022. Exploring *Bacillus thuringiensis* as a model for endospore adhesion
541 and its potential to investigate adhesins in *Pasteuria penetrans*. *J Appl Microbiol* 132:4371–4387.
- 542 45. Giorno R, Bozue J, Cote C, Wenzel T, Moody K-S, Mallozzi M, Ryan M, Wang R, Zielke R, Maddock JR,
543 Friedlander A, Welkos S, Driks A. 2007. Morphogenesis of the *Bacillus anthracis* Spore. *J Bacteriol* 189:691–
544 705.

- 545 46. Thompson BM, Hsieh H-Y, Spreng KA, Stewart GC. 2011. The co-dependence of BxpB/ExsFA and BclA for
546 proper incorporation into the exosporium of *Bacillus anthracis*: Co-dependence of BxpB and BclA. *Mol*
547 *Microbiol* 79:799–813.
- 548 47. Tan L, Turnbough CL. 2010. Sequence Motifs and Proteolytic Cleavage of the Collagen-Like Glycoprotein BclA
549 Required for Its Attachment to the Exosporium of *Bacillus anthracis*. *J Bacteriol* 192:1259–1268.
- 550 48. Bao S, Yu S, Guo X, Zhang F, Sun Y, Tan L, Duan Y, Lu F, Qiu X, Ding C. 2015. Construction of a cell-surface
551 display system based on the N-terminal domain of ice nucleation protein and its application in identification
552 of *mycoplasma* adhesion proteins. *J Appl Microbiol* 119:236–244.
- 553 49. Jung H-C, Lebeault J-M, Pan J-G. 1998. Surface display of *Zymomonas mobilis* levansucrase by using the ice-
554 nucleation protein of *Pseudomonas syringae*. *Nat Biotechnol* 16:576–580.
- 555 50. Park T, Heo N, Yim S, Park J, Jeong K, Lee S. 2013. Surface display of recombinant proteins on *Escherichia coli*
556 by BclA exosporium of *Bacillus anthracis*. *Microb Cell Factories* 12:81.
- 557 51. Ebert D, Zschokke-Rohringer CD, Carius HJ. 1998. Within–and between–population variation for resistance of
558 *Daphnia magna* to the bacterial endoparasite *Pasteuria ramosa*. *Proc R Soc Lond B Biol Sci* 265:2127–2134.
- 559 52. Sheppard AE, Poehlein A, Rosenstiel P, Liesegang H, Schulenburg H. 2013. Complete Genome Sequence of
560 *Bacillus thuringiensis* Strain 407 Cry-. *Genome Announc* 1:e00158-12, 1/1/e00158-12.
- 561 53. Monk IR, Shah IM, Xu M, Tan M-W, Foster TJ. 2012. Transforming the Untransformable: Application of Direct
562 Transformation To Manipulate Genetically *Staphylococcus aureus* and *Staphylococcus epidermidis*. *mBio* 3.
- 563 54. Janes BK, Stibitz S. 2006. Routine Markerless Gene Replacement in *Bacillus anthracis*. *Infect Immun* 74:1949–
564 1953.
- 565 55. Arnaud M, Chastanet A, Debarbouille M. 2004. New Vector for Efficient Allelic Replacement in Naturally
566 Nontransformable, Low-GC-Content, Gram-Positive Bacteria. *Appl Environ Microbiol* 70:6887–6891.
- 567 56. Gibson DG, Young L, Chuang R-Y, Venter JC, Hutchison CA, Smith HO. 2009. Enzymatic assembly of DNA
568 molecules up to several hundred kilobases. *Nat Methods* 6:343–345.
- 569 57. Tavares MB, Souza RD, Luiz WB, Cavalcante RCM, Casaroli C, Martins EG, Ferreira RCC, Ferreira LCS. 2013.
570 *Bacillus subtilis* Endospores at High Purity and Recovery Yields: Optimization of Growth Conditions and
571 Purification Method. *Curr Microbiol* 66:279–285.
- 572 58. Sheppard AE, Poehlein A, Rosenstiel P, Liesegang H, Schulenburg H. 2013. Complete Genome Sequence of
573 *Bacillus thuringiensis* Strain 407 Cry-. *Genome Announc* 1:e00158-12.
- 574 59. Fredericksen M, Ameline C, Krebs M, Hüßy B, Fields PD, Andras JP, Ebert D. 2021. Infection phenotypes of a
575 coevolving parasite are highly diverse, structured, and specific. *Evolution* 75:2540–2554.
- 576 60. Zhao X, Wang Y, Shang Q, Li Y, Hao H, Zhang Y, Guo Z, Yang G, Xie Z, Wang R. 2015. Collagen-Like Proteins
577 (ClpA, ClpB, ClpC, and ClpD) Are Required for Biofilm Formation and Adhesion to Plant Roots by *Bacillus*
578 *amyloliquefaciens* FZB42. *PLOS ONE* 10:e0117414.
- 579 61. Carrera M, Zandomeni RO, Fitzgibbon J, Sagripanti J-L. 2007. Difference between the spore sizes of *Bacillus*
580 *anthracis* and other *Bacillus* species. *J Appl Microbiol* 102.
- 581 62. Maes E, Krzewinski F, Garenaux E, Lequette Y, Coddeville B, Trivelli X, Ronse A, Faille C, Guerardel Y. 2016.
582 Glycosylation of BclA Glycoprotein from *Bacillus cereus* and *Bacillus anthracis* Exosporium Is Domain-specific.
583 *J Biol Chem* 291:9666–9677.
- 584 63. Waller LN, Stump MJ, Fox KF, Harley WM, Fox A, Stewart GC, Shahgholi M. 2005. Identification of a Second
585 Collagen-Like Glycoprotein Produced by *Bacillus anthracis* and Demonstration of Associated Spore-Specific
586 Sugars. *J BACTERIOL* 187:6.
- 587 64. Geyer H, Geyer R. 2006. Strategies for analysis of glycoprotein glycosylation. *Biochim Biophys Acta BBA -*
588 *Proteins Proteomics* 1764:1853–1869.
- 589 65. Duncan C, Prashar A, So J, Tang P, Low DE, Terebiznik M, Guyard C. 2011. Lcl of *Legionella pneumophila* Is an
590 Immunogenic GAG Binding Adhesin That Promotes Interactions with Lung Epithelial Cells and Plays a Crucial
591 Role in Biofilm Formation. *Infect Immun* 79:2168–2181.
- 592 66. Ellison AJ, Dempwolff F, Kearns DB, Raines RT. 2020. Role for Cell-Surface Collagen of *Streptococcus*
593 *pyogenes* in Infections 20.
- 594
595